Temporary Anion States of Ferrocene and Dibenzene Chromium Using Stabilization Method in Density Functional Theory

Hsiu-Yao Cheng,* Chun-Chi Shih, and Jung-Tzu Chang

Department of Chemistry, Tunghai University, Taichung 40704, Taiwan

Received: May 1, 2009; Revised Manuscript Received: June 21, 2009

The Koopmans-based (KB) approximation is used to investigate the ionization potentials of ferrocene and dibenzene chromium in density functional theory. As to the energies of low-lying temporary anion states of these transition metal complexes, the stabilization method coupled with KB approximation (S-KB) is adopted. Here, the stabilization is accomplished by varying the exponents of appropriate diffuse functions. Results indicate that the S-KB method is much more successful than other methods in predicting absolute and relative energies of temporary anion states. Furthermore, the ionization potentials via KB approach are very close to the experimental values.

1. Introduction

The determination of ionization potentials (IPs) and electron affinities (EAs) of molecules is important in the studies of chemical properties such as chemical reactivity, hardness, softness, electronegativity, and nonlinear optical activity. It is also imperative to understand the electron interactions with biologically molecules such as proteins or DNA, the electron transfer (ET) and hole transfer (HT) processes in donor-bridge-acceptor (D-B-A) compounds, and the electronic processes in molecular electronics.[1−10] The IPs and EAs can be separately determined by means of photoelectron spectroscopy (PES)[11] and electron transmission spectroscopy (ETS)[12,13] experimentally. In the theoretical prediction of IPs and EAs, the most widely used expression is the Koopmans' theorem (KT)[14] approximation using Hartree−Fock (HF) or Kohn−Sham (KS) orbital energies. The IPs and EAs in the KT approximation can be associated with the negatives of the energies of the filled and unfilled orbitals, respectively. However, this approximation neglects relaxation and correlation effects. Since correlation effects tend to oppose the electronic relaxation energy contribution for IPs but augment it for EAs, the KT approach generally predicts more reliable IPs than EAs.

The special difficulty of using the KT approximation in density functional theory (DFT)[15] method is due to a fundamental deficiency in the potentials of conventional continuum functional. Recently, Tozer and co-workers have proposed an alternative Koopmans-based (KB) approximation based on the consideration of the integer discontinuity (Δ_{xc}) in the exact exchange-correlation potential.[16−21] The applications by Tozer et al. have been shown to give improvement over other approaches for systems with large negative EAs. However, for species with negative EAs, the temporary anion is unstable with respect to electron detachment. Thus, the unfilled orbitals are prone to collapse onto approximations of continuum functions called orthogonalized discrete continuum (ODC)[22−25] when large basis sets are used. Therefore, the energy calculations of temporary anion states using both the KB and KT approaches cannot be considered definitive.

To distinguish the temporary anion orbital solutions from the ODC solutions, we have applied the stabilized Koopmans' theorem (S-KT) method (i.e., the stabilization method[26−29] coupled with KT)[30] and the S-KB method[31] to study the π^* temporary anion states of a series of substituted benzenes. Results indicate that both approaches are able to yield accurate relative energies of π^* states for substituted benzenes. However, the recently proposed S-KB approach can provide much better predictions in the absolute energies of π^* states as compared to the S-KT method.

As to transition-metal complexes, it is well-known that the DFT method is especially useful in describing their structures and properties. Yet, the stability of their temporary anion resonances has not been systematically examined. Hence, it is worthwhile to investigate the transition-metal complexes via the S-KB method. In this study, we will focus on the two prototypical sandwich compounds, ferrocene ($Fe(Cp)_2$) and dibenzene chromium (DBC). These compounds have been studied previously by the multiple scattering Xα (MS-Xα) method.[32−34] The results there have indicated that the temporary anion resonances are mainly from the d metal orbitals and the π or π^* orbitals of the rings. However, several important issues still remain unresolved concerning the temporary anion resonances using the Xα method.[35] For instance, stabilization of the temporary anion states via MS-Xα method was not established for the transition-metal complexes. Hence, it is fitting for us to apply S-KB approach to study the temporary anion resonances for ferrocene and DBC. As to the filled molecular orbitals, we will also apply the improved KB approximation to the IPs. Finally, the results obtained will be compared with other approaches.

2. Computational Methods

The IPs and EAs in the KT approximation can be expressed as

$$\mathrm{IP}^{\mathrm{KT}} \approx -\varepsilon_{\mathrm{OMO}} \tag{1}$$

and

$$\mathrm{EA}^{\mathrm{KT}} \approx -\varepsilon_{\mathrm{VMO}} \tag{2}$$

where $\varepsilon_{\mathrm{OMO}}$ and $\varepsilon_{\mathrm{VMO}}$ denote the occupied and virtual molecular orbital energies, respectively. When the alternative KB approxima-

* To whom correspondence should be addressed. E-mail: hycheng@thu.edu.tw. Phone: 011-886-4-23590248-102. Fax: 011-886-4-23590426.

10.1021/jp904056q CCC: $40.75
Published on Web 07/31/2009

TABLE 1: Calculated IPs (eV) for Ferrocene and Dibenzene Chromium

		ferrocene					dibenzene chromium				
method	basis set	e_{2g}	a_{1g}	e_{1u}	e_{1g}	d^c/eV	a_{1g}	e_{2g}	e_{1g}	e_{1u}	d^c/eV
KB^{PBEPBE}	A1	6.64	6.98	8.63	9.24	0.18	5.29	6.45	9.35	9.48	0.18
	A3	6.62	6.88	8.78	9.32	0.18	5.09	6.50	9.45	9.62	0.17
	B1	6.64	6.98	8.63	9.24	0.18	5.29	6.45	9.35	9.48	0.18
	C1	6.78	7.08	8.70	9.30	0.08	5.44	6.57	9.38	9.51	0.15
	C3	6.72	6.97	8.79	9.33	0.13	5.32	6.58	9.42	9.58	0.15
	C4	6.73	6.99	8.73	9.28	0.12	5.36	6.55	9.38	9.54	0.16
	D1	6.81	7.09	8.73	9.31	0.07	5.45	6.60	9.40	9.54	0.14
$KB^{TPSSTPSS}$	D1	6.64	7.14	8.54	9.11	0.19	5.46	6.41	9.24	9.41	0.19
KB^{VSXC}	D1	6.63	7.10	8.51	9.04	0.23	5.51	6.38	9.25	9.43	0.21
KT^{HF}	A1	11.72	13.97	9.10	9.24		9.78	6.45	9.66	10.40	
	C1	11.71	13.92	9.17	9.26		9.85	6.58	9.72	10.49	
$X\alpha$[a]		8.5	7.9	9.3	9.7		5.5	6.5	9.3	9.4	
Expt[b]		6.86	7.23	8.72	9.38		5.45	6.46	9.56	9.80	

[a] The IPs for $Fe(cp)_2$ and $Cr(C_6H_6)_2$ are obtained from previous studies.[42,43] [b] The experimental IPs for $Fe(cp)_2$ and $Cr(C_6H_6)_2$ are obtained from previous studies.[43,44] [c] d denotes the mean error relative to experimental IP data.

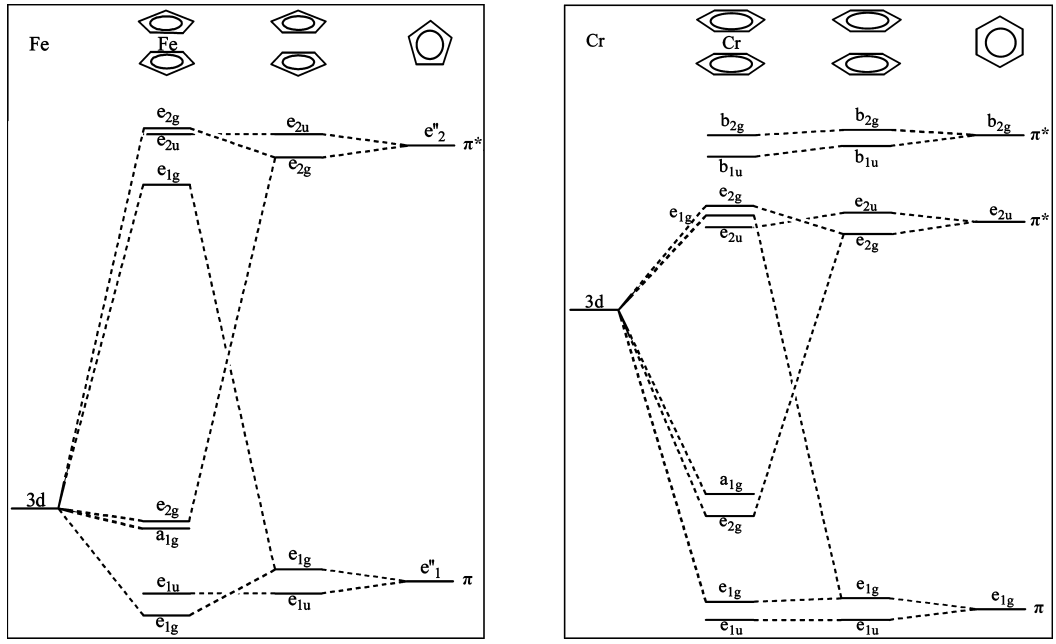

Figure 1. Correlation diagram of the frontier MOs in ferrocene and dibenzene chromium.

tion is applied, the correction of the Koopmans value is approximately half the integer discontinuity

$$\frac{\Delta_{xc}}{2} \approx \varepsilon_{\mathrm{HOMO}} + (E_{N-1} - E_N) \tag{3}$$

Here, $\varepsilon_{\mathrm{HOMO}}$ is the highest-occupied molecular orbital (HOMO) energy determined from a DFT calculation using a local exchange-correlation functional on the neutral system. E_N and E_{N-1} are the total electronic energies of the neutral and cation, respectively. By adding the correction term $\Delta_{xc}/2$ and $-\Delta_{xc}/2$ to IP^{KT} and EA^{KT}, respectively, the IP and EA in the KB approximation become

$$\mathrm{IP}^{\mathrm{KB}} \approx -\varepsilon_{\mathrm{OMO}} + [\varepsilon_{\mathrm{HOMO}} + (E_{N-1} - E_N)] \tag{4}$$

and

$$\mathrm{EA}^{\mathrm{KB}} \approx -\varepsilon_{\mathrm{VMO}} - [\varepsilon_{\mathrm{HOMO}} + (E_{N-1} - E_N)] \tag{5}$$

The vertical attachment energy, i.e., the negative of EA, can then be represented as

$$\mathrm{AE}^{\mathrm{KB}} \approx \varepsilon_{\mathrm{VMO}} + [\varepsilon_{\mathrm{HOMO}} + (E_{N-1} - E_N)] \tag{6}$$

The virtual orbital energy associated with temporary anion state is also known as AE. The AE obtained from KB approach in eq 6 will be denoted as $\varepsilon_{\mathrm{VMO}}^{\mathrm{KB}}$.

The stabilization method is employed to distinguish the temporary anion state solutions from the virtual ODC solutions. Eight different Gaussian-type basis sets, designated as A1, A3, B1, C1, C2, C3, C4, and D1, are employed for our calculations. The convention of designation is as follows. For the C atom, the 6-31G+αp_1 basis set A is formed by augmenting the 6-31G basis set with the diffuse p_1 function multiplied by a scale factor α (denoted by αp_1). The 6-31G+$\alpha(p_1+p_2)$ basis set B is formed by augmenting the 6-31G basis set with the αp_1 and αp_2 diffuse functions. The p_1 and p_2 functions have the exponents of 0.0562 and 0.0187, respectively. The 6-31+G(d)+αp_3 basis set C is formed by augmenting the 6-31+G(d) basis set with the

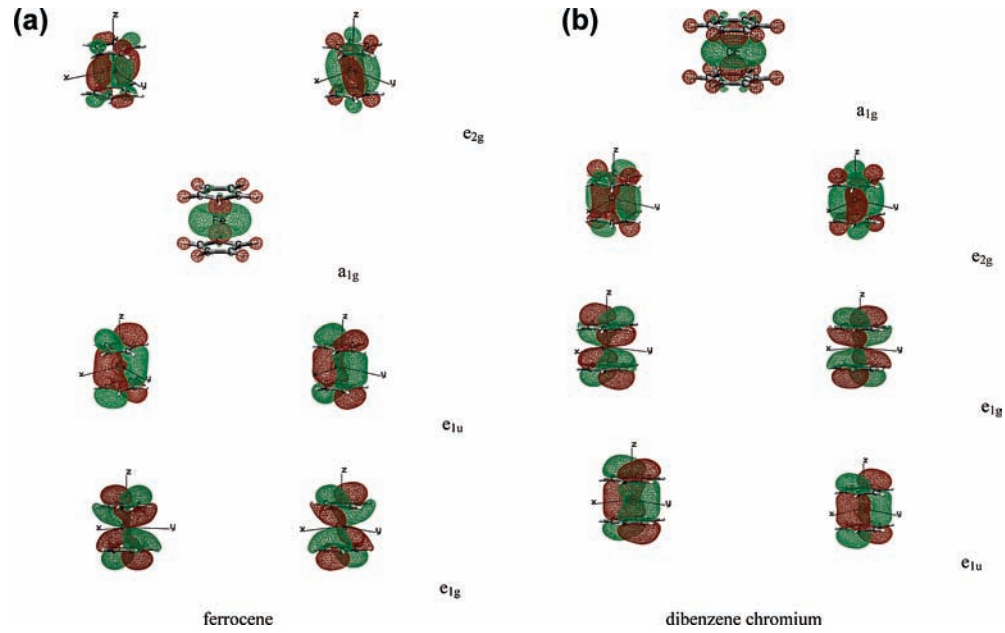

Figure 2. Plots of the frontier filled MOs for (a) ferrocene and (b) dibenzene chromium. The isosurface values are chosen to be 0.02 for all the MO plots.

diffuse αp_3 function. The p_3 functions have the exponents of 0.0146. The aug-cc-pvdz+αp_4 basis set D is formed by augmenting the aug-cc-pvdz basis set with the diffuse αp_4 function. The p_4 functions have the exponents of 0.0135. For Fe and Cr atoms, the following four different Gaussian-type basis sets 1−4 are employed, and they are denoted alongside with A−D basis sets. (1) The akr45+αd_1 basis set is formed by augmenting the (13s10p5d)/[5s4p2d] akr45 basis set of Rappe, Smedley, and Goddard[36] with the diffuse αd_1 function. The diffuse d_1 functions have the exponents of 0.0704 and 0.054 for the Fe and Cr atoms, respectively. (2) The akr45+$\alpha(d_1+d_2)$ basis set is formed by augmenting the akr45 basis set with the αd_1 and αd_2 diffuse functions. The diffuse d_2 functions have the exponents of 0.0235 and 0.018 for the Fe and Cr atoms, respectively. (3) The 6-31G+αd_3 basis set is formed by augmenting the 6-31G basis set with the αd_3 diffuse function. The diffuse d_3 functions have the exponents of 0.1681 and 0.1335 for the Fe and Cr atoms, respectively. (4) The 6-31+G(d)+αd_4 basis set is formed by augmenting the 6-31+G(d) basis set with the αd_4 diffuse function. The diffuse d_4 functions have the exponents of 0.0378 and 0.0304 for the Fe and Cr atoms, respectively. To sum up, the basis set "Xn" represents both the basis set X (X = A, B, C, or D) for the C atom and n (n = 1, 2, 3, or 4) for the Fe or Cr atoms.

As α increases, the ODC solutions may approach the temporary anion state orbital solutions in energy and lead to avoided crossing between the two types of solutions. The stabilization graphs are obtained by plotting the calculated energies (ε_{VMO}^{KB}) as a function of the scale factor α. The energy of the anion shape resonance is taken as the mean value of the two eigenvalues involved in the avoided crossing at their point of closest approach α_{ac} if the avoided crossing occurs between temporary anion and ODC solution.[37]

In the present study, we will use the PBEPBE method[38] which utilizes pure generalized gradient approximation (GGA) functional as in the works of Tozer and co-workers. As for comparison, two meta GGA (MGGA) functional TPSSTPSS[39] and VSXC[40] using D1 basis set will also be studied. The HF method is also employed. All calculations are performed using the Gaussian 03 program.[41] The geometries of the neutral ferrocene and DBC molecules are optimized at the B3LYP/6-31+G* level under D_{5d} and D_{6h} symmetry constraints, respectively. The symmetry in the labeling of the orbital is based on the convention that the principal axis is along the z-axis.

3. Results and Discussion

We perform KB calculations using PBEPBE (KB^{PBEPBE}), TPSSTPSS ($KB^{TPSSTPSS}$), VSXC (KB^{VSXC}), and KT calculations using HF method (KT^{HF}) on the filled orbitals for ferrocene and DBC. The calculated IPs are tabulated along with the experimental values in Table 1. In the KB^{PBEPBE} method, the first IPs are due to ionization from the e_{2g} for ferrocene and a_{1g} for DBC, respectively. The increasing order of IPs of filled MOs are $e_{2g} < a_{1g} < e_{1u} < e_{1g}$ for ferrocene and $a_{1g} < e_{2g} < e_{1g} < e_{1u}$ for DBC. The calculated IPs using the KB^{PBEPBE} methods are in very good agreement with the experimental values as can be seen from Table 1. The range of errors as compared with experimental values is within 0.2 eV for all basis sets. For the $KB^{TPSSTPSS}$ and KB^{VSXC} method, the errors for IPs (0.19−0.23 eV) are slightly larger than those (0.07−0.14 eV) of the KB^{PBEPBE} method when the D1 basis set is used. As to the KT calculations, none of them has generated accurate IPs. In Table 1, only the representative results of A1 and C1 basis sets are tabulated. As can be seen from the data, the values are far off as compared with experimental ones. Notice that if Xα method is used for ferrocene, its errors for IPs are larger than those of the KB^{PBEPBE} method. Moreover, the order of IPs is not conformable with ours. It is clear that the KB^{PBEPBE} approach so far has the best prediction in IPs among these approaches.

We then examine the characteristics of MOs using KB^{PBEPBE} method. The correlation diagrams of the frontier MOs of ferrocene and DBC are illustrated in Figure 1. The 3d orbitals of metal yield a_{1g} (d_{z^2}), e_{2g} ($d_{x^2-y^2,xy}$), and e_{1g} ($d_{xz,yz}$) orbitals in the D_{5d}/D_{6h} point group. The empty cyclopentadienyl (Cp) e''_2 (π^*) orbitals correlate with orbitals of e_{2g} and e_{2u} symmetry and the filled (Cp) e''_1 (π) orbitals correlate with

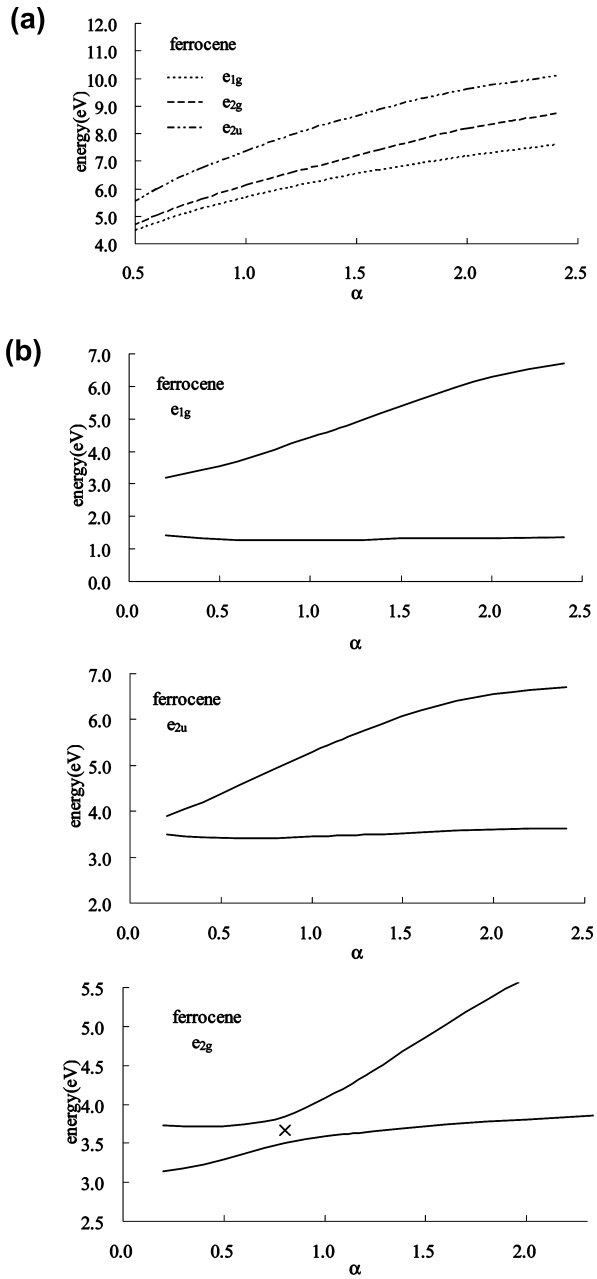

Figure 3. (a) Energies of e_{1g}, e_{2u}, and e_{2g} virtual orbitals of ferrocene as a function of the scaling factor α for a free electron in the absence of potentials. (b) Stabilization graphs for ferrocene. Energies of e_{1g}, e_{2u}, and e_{2g} virtual orbitals as a function of α. The location of α_{ac} is marked with ×.

orbitals of e_{1u} and e_{1g} symmetry on $Fe(Cp)_2$. Similarly, the empty benzene e_{2u} (π^*) orbitals correlate with orbitals of e_{2g} and e_{2u} symmetry; b_{2g} (π^*) orbitals correlate with orbitals of b_{1u} and b_{2g} symmetry, and the filled benzene e_{1g} (π) orbitals correlate with orbitals of e_{1u} and e_{1g} symmetry on DBC. The filled MOs for ferrocene and DBC using basis set A1 are illustrated in parts a and b of Figure 2. As indicated in Figure 2a for ferrocene, occupied e_{2g} orbitals are the HOMOs. The orbitals result from the mixing of $(Cp)_2$ π^* orbitals with Fe ($d_{x^2-y^2,xy}$). The MO a_{1g} is essentially Fe(d_{z^2}), and the e_{1u} orbitals are mainly from the $(Cp)_2$ π orbitals. The e_{1g} orbitals correspond to π-bonding interaction between $(Cp)_2$ π orbitals and Fe ($d_{xz,yz}$). For DBC, the a_{1g} orbital is the HOMO. Its main contribution comes from Cr(d_{z^2}). The e_{2g} orbitals are resulted from the mixing of $(C_6H_6)_2$ e_{2g} π^* orbitals with Cr ($d_{x^2-y^2,xy}$). The e_{1u} orbitals correspond to the $(C_6H_6)_2$ e_{1u} π orbitals, and the e_{1g} orbitals correspond to π-bonding interaction between Cr ($d_{xz,yz}$) and $(C_6H_6)_2$ π orbitals.

For the temporary anion states, we perform S-KB calculations on the unfilled orbitals to distinguish them from the ODC solutions via the PBEPBE, TPSSTPSS, and VSXC (S-KB^{PBEPBE}, S-$KB^{TPSSTPSS}$, S-KB^{VSXC}) and then the S-KT for the HF methods (S-KT^{HF}). First, we will present the results of S-KB^{PBEPBE}. Figure 3a shows the energies of the discrete continuum (DC)[22−25] solutions as a function of scale factor α for the e_{1g}, e_{2u}, and e_{2g} virtual orbitals of ferrocene using the basis set A1. The energies of the DC solutions are obtained by solving the KS equation for a free electron in the absence of any potential. The stabilization graphs of the energies as a function of α for the e_{1g}, e_{2u}, and e_{2g} virtual states of ferrocene using basis set A1 are shown in Figure 3b, respectively. There are two types of energies for virtual orbital solutions in the S-KB calculations. One is the unfilled orbital solution and the other the ODC virtual orbital solution. The unfilled orbital solution and the ODC solutions are readily distinguished by examining how their energies vary with α. As shown in Figure 3b, the first solutions that remain stabilized with α are the e_{1g} and e_{2u} orbital solutions, and the stabilized energy values are 1.34 and 3.56 eV, respectively. Because of the characteristics of bound-state-like solution for the temporary anion state, the independence of the energy eigenvalues with respect to α will persist even to very diffuse basis sets. The other solutions that are appreciably higher in energies than the resonance solution correspond to the ODC solutions. In general, the calculations will fail if the values of α are too small (usually $\alpha < 0.2$). Notice that the VMO eigenvalues for a free electron are always positive. Hence, when the calculated VMO eigenvalues of virtual state are much smaller than 0 ($\varepsilon_{VMO} < 0$), the energies of ODC solutions will be higher than those of the virtual state. Consequently, no avoided crossings will be found for all α in the stabilization graphs. For instance, the e_{1g} virtual states of ferrocene will not be observed even when the calculations are extended to smaller α values.

Note that the energies of ODC lie below that of the DC when S-KB method in DFT is used. However, the opposite can be true if different approaches, such as SKT-HF or S-ΔMP2, are used.[22,45] Possible reasons for this discrepancy are due to the different considerations of exchange-correlation potential and self-interaction effect.[46,47] For the e_{2g} virtual states in Figure 3b, the first and second solutions undergo an avoided crossing at $\alpha_{ac} = 0.8$. The energy of the e_{2g} orbitals is 3.67 eV at $\alpha_{ac} = 0.8$. By analysis of the nature of virtual orbitals, the first solution for $\alpha < 0.8$ and the second solution for $\alpha > 0.8$ are from the ODC solution. On the other hand, the second solution for $\alpha < 0.8$, and the first solution for $\alpha > 0.8$ are mainly from the e_{2g} resonance solution.

The first and second e_{1g}, e_{2u}, and e_{2g} virtual orbitals of ferrocene for $\alpha = 2.0$ ($> \alpha_{ac}$) are displayed in parts a and b of Figure 4. Here, the value $\alpha = 2.0$ can be arbitrarily chosen as long as it is greater than α_{ac}. The first virtual orbitals correspond to the resonance solutions. The second virtual orbitals containing extra diffuse function character are from ODC solutions. As can be seen in Figures 1 and 4a, the e_{1g} orbitals correspond to π-antibonding interaction between $(Cp)_2$ π orbitals and Fe ($d_{xz,yz}$). The e_{2u} orbitals are essentially derived from the $(Cp)_2$ π^* orbitals. The e_{2g} orbitals are resulted from the antibonding interaction between $(Cp)_2$ π^* orbitals and Fe ($d_{x^2-y^2}$,d_{xy}).

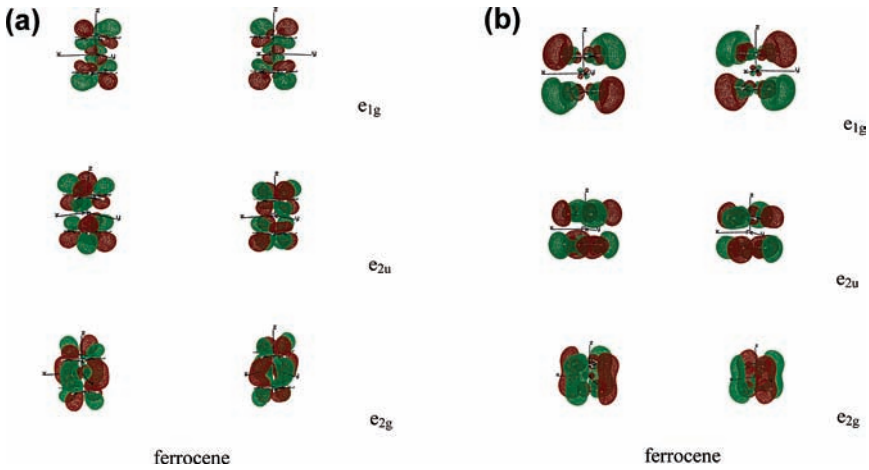

Figure 4. Plots of the (a) first and (b) second e_{1g}, e_{2u}, and e_{2g} virtual orbitals at $\alpha = 2.0$ for ferrocene. The isosurface values are chosen to be 0.02 for all the MO plots.

TABLE 2: Calculated[a] and Corrected[b] AEs (eV) for Ferrocene and Dibenzene Chromium

		ferrocene				dibenzene chromium					
method	basis set	e_{1g}	e_{2u}	e_{2g}	d[d] /eV	e_{2u}	e_{1g}	e_{2g}	b_{1u}	b_{2g}	d[d]/eV
S-KB[PBEPBE]	A1	1.34	3.56	3.67	0.82	1.69	2.16	2.90	4.44	5.49	0.84
		(0.63	2.85	2.96)		(0.76	1.23	1.99	3.51	4.56)	
	A3	1.32	3.56	3.56	0.78	1.75	2.22	2.95	4.57	5.26	0.85
		(0.63	2.87	2.87)		(0.76	1.23	1.96	3.58	4.27)	
	B1	1.27	3.42	3.59	0.72	1.67	2.00	2.73	4.36	5.30	0.71
		(0.63	2.78	2.95)		(0.76	1.09	1.82	3.45	4.39)	
	C1	1.14	3.24	3.26	0.51	1.47	1.77	2.48	4.19	5.42	0.57
		(0.63	2.73	2.75)		(0.76	1.06	1.77	3.48	4.71)	
	C2	1.15	3.25	3.28	0.52	1.48	1.78	2.49	4.19	5.35	0.56
		(0.63	2.73	2.76)		(0.76	1.06	1.77	3.47	4.63)	
	C3	1.15	3.17	3.27	0.49	1.42	1.79	2.46	4.15	5.29	0.52
		(0.63	2.65	2.75)		(0.76	1.13	1.80	3.49	4.63)	
	C4	1.19	3.19	3.27	0.51	1.39	1.82	2.49	4.13	5.24	0.51
		(0.63	2.63	2.71)		(0.76	1.19	1.86	3.50	4.61)	
	D1	1.09	3.14	3.15	0.42	1.37	1.70	2.37	4.03	5.13	0.42
		(0.63	2.68	2.69)		(0.76	1.09	1.76	3.42	4.52)	
S-KB[TPSSTPSS]	D1	1.18	3.23	3.25	0.52	1.49	1.94	2.49	4.25	5.47	0.63
		(0.63	2.68	2.70)		(0.76	1.21	1.76	3.52	4.74)	
S-KB[VSXC]	D1	1.02	3.23	3.22	0.45	1.45	1.87	2.33	4.22	5.37	0.55
		(0.63	2.84	2.83)		(0.76	1.18	1.64	3.53	4.68)	
KT[PBEPBE]	A1	−1.23	1.04	1.39	1.64	−0.63	−0.19	0.57	2.20	3.15	1.48
		(0.63	2.90	3.25)		(0.76	1.20	1.96	3.59	4.54)	
	A3	−1.21	0.89	1.32	1.70	−0.71	−0.07	0.60	2.12	3.08	1.50
		(0.63	2.73	3.16)		(0.76	1.40	2.07	3.59	4.55)	
	B1	−1.23	1.04	1.39	1.64	−0.63	−0.19	0.57	2.20	3.15	1.48
		(0.63	2.90	3.25)		(0.76	1.20	1.96	3.59	4.54)	
	C1	−1.51	0.60	0.59	2.14	−0.96	−0.64	0.08	1.45	2.27	2.06
		(0.63	2.74	2.73)		(0.76	1.08	1.80	3.17	3.99)	
	C3	−1.47	0.53	0.55	2.17	−1.03	−0.60	0.08	1.41	2.22	2.08
		(0.63	2.63	2.65)		(0.76	1.19	1.87	3.20	4.01)	
	C4	−1.44	0.57	0.59	2.13	−1.01	−0.58	0.09	1.43	2.26	2.06
		(0.63	2.64	2.66)		(0.76	1.19	1.86	3.20	4.03)	
	D1	−1.56	0.52	0.40	2.25	−1.04	−0.70	−0.03	1.07	1.87	2.27
		(0.63	2.71	2.59)		(0.76	1.10	1.77	2.87	3.67)	
S-KT[HF]	A1	6.21	5.95	5.24	3.77	3.72	8.13	5.94	3.96	4.68	2.79
		(1.60	1.34	0.63)		(0.76	5.17	2.98	1.00	1.72)	
	C1	6.10	5.78	5.34	3.71	3.62	7.89	5.21	4.16	4.49	2.57
		(1.39	1.07	0.63)		(0.76	5.03	2.35	1.30	1.63)	
KT[HF]	A1	6.79	6.02	6.26	4.33	3.78	7.89	12.12	7.86	5.67	4.96
		(1.40	0.63	0.87)		(0.76	4.87	9.10	4.84	2.65)	
	C1	2.64	4.32	3.15	1.33	6.28	2.64	2.46	3.16	3.79	1.17
		(0.63	2.31	1.14)		(4.58	0.94	0.76	1.46	2.09)	
Xα[c]		1.26	2.78	2.94		1.5	1.2	1.9	3.7	4.9	
Expt[c]		0.63	2.74			0.76	1.22	1.93	3.80	4.79	

[a] The energies of the HOMO (ε_{HOMO}) in eq 5 are calculated for each value of α even though the variations of ε_{HOMO} values are within 0.1 eV. [b] The corrected values (shown in parentheses) are obtained by subtracting the amount of bias needed to bring the calculated AEs into agreement with experimental values for the lowest anion state of ferrocene/dibenzene chromium. [c] The AEs for $Fe(cp)_2$ and $Cr(C_6H_6)_2$ are obtained from refs 32 and 34, respectively. [d] d denotes the mean error relative to experimental AE data.

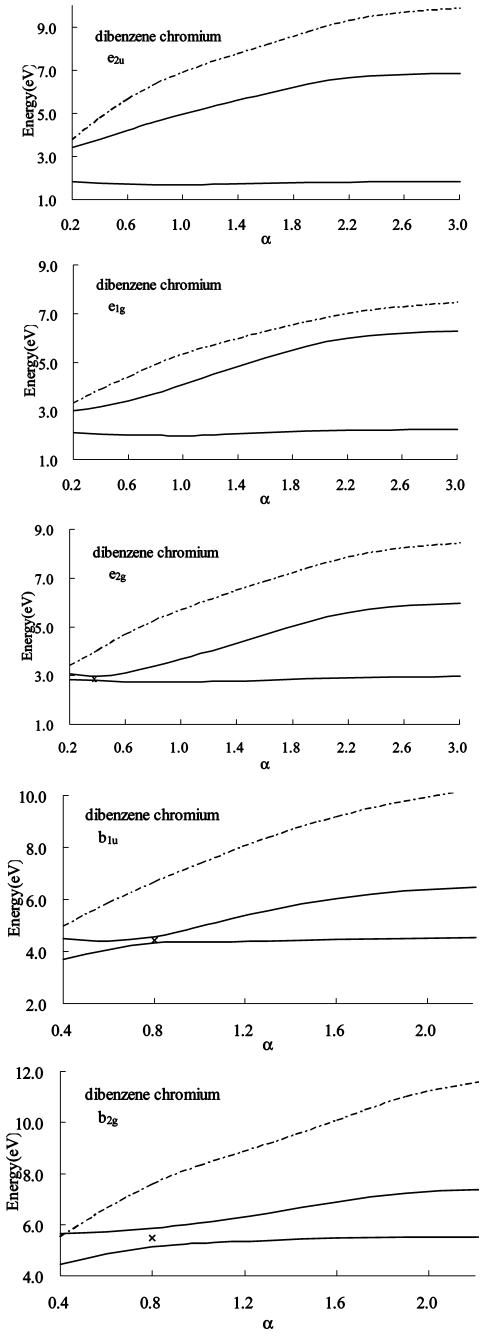

Figure 5. Stabilization graphs for dibenzene chromium. Energies of e_{2u}, e_{1g}, e_{2g}, b_{1u}, and b_{2g} virtual orbitals (represented by the solid curves) and the free electron (represented by the dashed curves) as a function of α. The location of α_{ac} is marked with ×.

The stabilization graphs of energies as a function of α for the e_{2u}, e_{1g}, e_{2g}, b_{1u}, and b_{2g} virtual states of DBC and the free electron using basis set A1 are shown in Figure 5. In this figure, the first solutions that remain stabilized with α are the e_{2u} and e_{1g} orbital solutions and the stabilized energy values are 1.69 and 2.16 eV, respectively. The other solutions that are appreciably higher in energies than the resonance solution correspond to the ODC solutions. For the e_{2g}, b_{1u}, and b_{2g} virtual states, the first and second solutions undergo an avoided crossing at α_{ac}. The energies of the e_{2g}, b_{1u}, and b_{2g} orbitals are 2.90 eV at $\alpha_{ac} = 0.4$, 4.44 eV at $\alpha_{ac} = 0.8$, and 5.49 eV at $\alpha_{ac} = 0.8$, respectively. The first and second e_{2u}, e_{1g}, e_{2g}, b_{1u}, and b_{2g} virtual orbitals of DBC for $\alpha = 2.0$ are illustrated in parts a and b of Figure 6. As indicated in this figure, the first virtual orbitals correspond to resonance solutions and the second virtual orbitals correspond to ODC solutions. According to Figures 1 and 6a, the e_{2u} orbitals, the LUMOs, are essentially from $(C_6H_6)_2$ e_{2u} π^* orbitals. The e_{1g} orbitals are mainly from the mixing of Cr ($d_{xz,yz}$) with $(C_6H_6)_2$ e_{1g} π orbitals. The e_{2g} orbitals correspond to antibonding interaction between $(C_6H_6)_2$ π^* orbitals and Cr ($d_{x2-y2,xy}$). Both b_{1u} and b_{2g} orbitals are derived from $(C_6H_6)_2$ π^*orbitals.

The stabilization graphs of energies using other basis sets are similar to those of A1. The results of AEs using various S-KB, S-KT, and KT methods are summarized in Table 2. To compare with experimental results, "corrected" AEs are also included in the table. The corrected values are obtained by subtracting an amount of bias denoted by b from the calculated AE values to bring the lowest anion state of ferrocene and DBC into agreement with the experimental values. For instance, when the basis set A1 is used, the values of b are 0.71 and 0.93 for ferrocene and DBC, respectively.

We will first discuss the results obtained from the PBEPBE method. Table 2 shows that the predicted order of unfilled MOs are the same when using the S-KB^{PBEPBE} and the KT^{PBEPBE} methods. The increasing order of AEs of unfilled MOs are $e_{1g} < e_{2u} < e_{2g}$ for ferrocene and $e_{2u} < e_{1g} < e_{2g} < b_{1u} < b_{2g}$ for DBC. For the results of S-KB^{PBEPBE} calculations, the mean errors for AEs are about 0.8 eV for the smaller A1 and A3 basis sets. When the larger D1 basis set is used, the AEs obtained are closer to experimental values. The mean errors for AEs relative to the experimental data are reduced to 0.4 eV for both molecules. There is almost no change in the results of AEs when the basis set is sufficient to span the space. However, the mean errors of AEs are greater than 1.5 eV when the KT^{PBEPBE} method is used. In Table 2, the mean errors for AEs are 2.2 and 2.3 eV for ferrocene and DBC with the D1 basis set, respectively. Hence, the S-KB^{PBEPBE} approach yields an improvement in the prediction of the absolute energies of temporary anion states over KT^{PBEPBE} approach.

As to the relative AEs (ΔAEs), Table 2 demonstrates that the S-KB^{PBEPBE} approach generates in general more accurate ΔAEs than those of the KT^{PBEPBE}. When using the larger basis sets C1−C4, the range of errors for ΔAEs between the LUMOs and the other anion states is within 0.2 eV as compared to experimental values. The errors may be derived from the inherent experimental uncertainties. For the broad resonance in ETS structures, the errors could be as large as 0.1 eV. As to the uncertainties in extracting the resonance energies from the stabilization graphs, they could also be as large as 0.1 eV.[35] Consequently, the S-KB approach can yield reasonable predictions of the relative energies of resonance states when using the flexible sizes of basis sets. In Table 2, it is found that the KT^{PBEPBE} calculations can sometimes account quantitatively for the ΔAEs. For instance, the average errors for ΔAEs between the $^2E_{1g}$-$^2E_{2u}$ and $^2E_{1g}$-$^2E_{2g}$ anion states for ferrocene with basis set C1 are within 0.1 eV. This fortuitous agreement is due to the fact that the three virtual orbitals in C1 are mainly from the resonance solutions.

In Table 2, the mean errors of AEs obtained by the S-KB^{TPSSTPSS} and S-KB^{VSXC} methods (0.45−0.63 eV) are slightly larger than those (0.42 eVs) of the S-KB^{PBEPBE} method with the D1 basis set. According to the table, we can see that none of the KT^{HF} and S-KT^{HF} methods can generate accurate absolute and relative AEs. The HF calculations lead to 1−5 eV errors for AEs. When using the Xα method for ferrocene, the mean errors for AEs and the

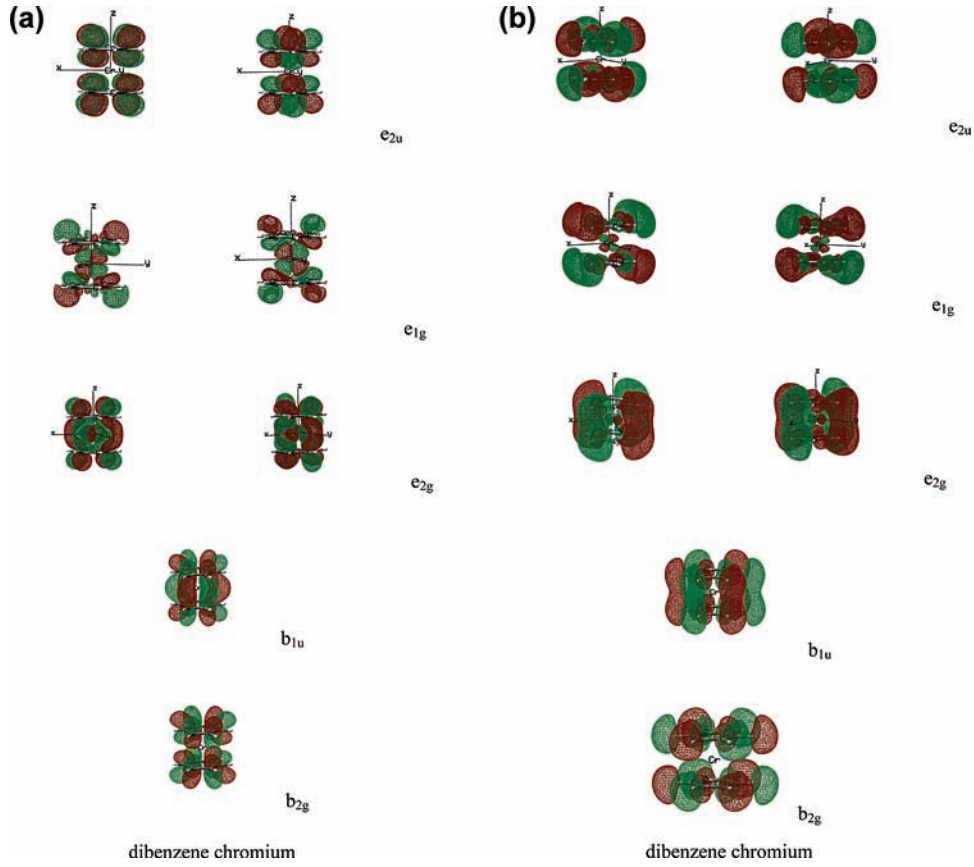

Figure 6. Plots of the (a) first and (b) second e_{2u}, e_{1g}, e_{2g}, b_{1u}, and b_{2g} virtual orbitals at $\alpha = 2.0$ for dibenzene chromium. The isosurface values are chosen to be 0.02 for all the MO plots.

average errors for ΔAEs between the $^2E_{1g}$-$^2E_{2u}$ and $^2E_{1g}$-$^2E_{2g}$ anion states for ferrocene are both about 0.5 eV. As for DBC, only the orders of unfilled e_{2u} and e_{1g} orbitals of DBC are not conformable with ours. The Xα method can be regarded as a special case of DFT using the local density approximation with the correlation functional omitted. The AEs are calculated by Slater's transition state method[48] with half an electron being added to an empty orbital. However, the AEs obtained from MS-Xα method are found to be quite sensitive to the sphere overlap used for the muffin-tin approximation (MTA). The drawback in the MTA of the potential often gives unreliable results in molecular calculation. Therefore, the S-KB method using modern DFT method should be more useful in studying the AEs of temporary anion states than the Xα method. It is worth noting that the long-range corrected density functional such as LC-wPBE,[49] CAM-B3LYP,[50] and wB97XD[51] provided by the latest Gaussian 09 or Q-Chem 3.2 program can also be adopted for future studies.

4. Conclusion

The energies of filled and unfilled orbitals in ferrocene and dibenzene chromium have been studied. Results have demonstrated that the KB approach using DFT method can yield very good results for IPs. The S-KB approach has yielded an improvement in predicting both the absolute and relative energies of temporary anion states over other approaches. The main reasons are (1) the adoption of stabilization method to distinguish the temporary anion solutions from the ODC ones and (2) the addition of asymptotic functional correction using KB method. It is believed that the KB and S-KB methods are particularly useful in determining IPs and EAs for transition metal complexes, respectively.

Acknowledgment. We would like to thank the reviewers for valuable comments during the revision process and National Center for High-Performance Computing for the computational resources provided. This work was supported by National Science Council of Republic of China.

References and Notes

(1) Simons, J. *J. Phys. Chem. A* **2008**, *112*, 6401.
(2) Lyngdoh, R. H. D.; Schaefer, H. F., III *Acc. Chem. Res.* **2009**, *42*, 563.
(3) Nitzan, A.; Ratner, M. A. *Science* **2003**, *300*, 1384.
(4) Jordan, K. D.; Paddon-Row, M. N. *Chem. Rev.* **1992**, *92*, 395.
(5) Jordan, K. D.; Paddon-Row, M. N. *J. Phys. Chem.* **1992**, *96*, 1188.
(6) Paddon-Row, M. N.; Jordan, K. D. *J. Am. Chem. Soc.* **1993**, *115*, 2952.
(7) Paddon-Row, M. N.; Shephard, M. J.; Jordan., K. D. *J. Phys. Chem.* **1993**, *97*, 1743.
(8) Mikkelsen, K. V.; Ratner, M. D. *Chem. Rev.* **1987**, *87*, 113.
(9) Newton, M. D. *Chem. Rev.* **1991**, *91*, 767.
(10) Scheer, A. M.; Aflatooni, K.; Gallup, G. A.; Burrow, P. D. *Phys. Rev. Lett.* **2004**, *92*, 068102.
(11) Rabalais, J. W. *Principles of Ultraviolet Photoelectron Spectroscopy*; John Wiley and Sons: New York, 1977.
(12) Sanche, L.; Schulz, G. J. *Phys. Rev. A* **1972**, *5*, 1672.
(13) Jordan, K. D.; Burrow, P. D. *Chem. Rev.* **1987**, *87*, 557.
(14) Koopmans, T. *Physica* **1934**, *1*, 104.
(15) Kohn, W.; Sham, L. J. *Phys. Rev. A* **1965**, *140*, 1133.
(16) Tozer, D. J.; De Proft, F. *J. Phys. Chem. A* **2005**, *109*, 8923.
(17) Tozer, D. J.; De Proft, F. *J. Chem. Phys.* **2007**, *127*, 034108.
(18) De Proft, F.; Sablon, N.; Tozer, D. J.; Geerlings, P. *Faraday Discuss.* **2007**, *135*, 151.
(19) Sablon, N.; De Proft, F.; Geerlingsa, P.; Tozer, D. J. *Phys. Chem. Chem. Phys.* **2007**, *9*, 5880.

(20) Teale, A. M.; De Proft, F.; Tozer, D. J. *J. Chem. Phys.* **2008**, *129*, 044110.
(21) Hajgató, B.; Deleuze, M. S.; Tozer, D. J.; De Proft, F. *J. Chem. Phys.* **2008**, *129*, 084308.
(22) Falcetta, M. F.; Jordan, K. D. *J. Phys. Chem.* **1990**, *94*, 5666.
(23) Falcetta, M. F.; Jordan, K. D. *J. Am. Chem. Soc.* **1991**, *113*, 2903.
(24) Burrow., P. D.; Howard., A. E.; Johnston., A. R.; Jordan., K. D. *J. Phys. Chem.* **1992**, *96*, 7570.
(25) Juang, C.-Y.; Chao, J. S.-Y. *J. Phys. Chem.* **1994**, *98*, 13506.
(26) Hazi, A. U.; Taylor, H. S. *Phys. Rev. A* **1970**, *1*, 1109.
(27) Taylor, H. S. *Adv. Chem. Phys.* **1970**, *18*, 91.
(28) Fels, M. F.; Hazi, A. U. *Phys. Rev. A* **1972**, *5*, 1236.
(29) Taylor, H. S.; Hazi, A. U. *Phys. Rev. A* **1976**, *14*, 2071.
(30) Chen, C.-S.; Feng, T.-H.; Chao, J. S.-Y. *J. Phys. Chem.* **1995**, *99*, 8629.
(31) Cheng, H.-Y.; Shih, C.-C. *J. Phys. Chem. A* **2009**, *113*, 1548.
(32) Modelli, A.; Foffani, A.; Guerra, M.; Jones, D.; Distefano, G. *Chem. Phys. Lett.* **1983**, *99*, 58.
(33) Giordan, J. C.; Moore, J. H.; Tossell, J. A.; Weber., J. *J. Am. Chem. Soc.* **1983**, *105*, 3431.
(34) Burrow, P. D.; Modelli, A.; Guerra, M.; Jordan, K. D. *Chem. Phys. Lett.* **1985**, *118*, 328.
(35) Chao, J. S.-Y.; Jordan, K. D. *J. Phys. Chem.* **1987**, *91*, 5578.
(36) Rappe, A. K.; Smedley, T. A.; Goddared, W. A., III *J. Phys. Chem.* **1981**, *85*, 2607.
(37) We use the simplest "midpoint method" adopted by Burrow et al. to extract resonance energy.[31]
(38) Perdew, J. P.; Burke, K.; Ernzerhof, M. *Phys. Rev. Lett.* **1996**, *77*, 3865.
(39) Tao, J. M.; Perdew, J. P.; Staroverov, V. N.; Scuseria, G. E. *Phys. Rev. Lett.* **2003**, *91*, 146401.
(40) Van Voorhis, T.; Scuseria, G. E. *J. Chem. Phys.* **1998**, *109*, 400.
(41) Frisch, M. J.; Trucks, G. W.; Schlegel, H. B.; Scuseria, G. E.; Robb, M. A.; Cheeseman, J. R.; Montgomery, J. A., Jr.; Vreven, T.; Kudin, K. N.; Burant, J. C.; Millam, J. M.; Iyengar, S. S.; Tomasi, J.; Barone, V.; Mennucci, B.; Cossi, M.; Scalmani, G.; Rega, N.; Petersson, G. A.; Nakatsuji, H.; Hada, M.; Ehara, M.; Toyota, K.; Fukuda, R.; Hasegawa, J.; Ishida, M.; Nakajima, T.; Honda, Y.; Kitao, O.; Nakai, H.; Klene, M.; Li, X.; Knox, J. E.; Hratchian, H. P.; Cross, J. B.; Bakken, V.; Adamo, C.; Jaramillo, J.; Gomperts, R.; Stratmann, R. E.; Yazyev, O.; Austin, A. J.; Cammi, R.; Pomelli, C.; Ochterski, J. W.; Ayala, P. Y.; Morokuma, K.; Voth, G. A.; Salvador, P.; Dannenberg, J. J.; Zakrzewski, V. G.; Dapprich, S.; Daniels, A. D.; Strain, M. C.; Farkas, O.; Malick, D. K.; Rabuck, A. D.; Raghavachari, K.; Foresman, J. B.; Ortiz, J. V.; Cui, Q.; Baboul, A. G.; Clifford, S.; Cioslowski, J.; Stefanov, B. B.; Liu, G.; Liashenko, A.; Piskorz, P.; Komaromi, I.; Martin, R. L.; Fox, D. J.; Keith, T.; Al-Laham, M. A.; Peng, C. Y.; Nanayakkara, A.; Challacombe, M.; Gill, P. M. W.; Johnson, B.; Chen, W.; Wong, M. W.; Gonzalez, C.; Pople, J. A. *Gaussian 03*, revision C.02; Gaussian, Inc.: Wallingford, CT, 2004.
(42) Rösch, N.; Johnson, K. H. *Chem. Phys. Lett.* **1974**, *24*, 179.
(43) Rabalais, J. W.; Werme, L. O.; Bergmak, T.; Karlson, L.; Hussain, M.; Siegbahn, K. *J. Chem. Phys.* **1972**, *57*, 1185.
(44) Guest, M. F.; Hillier, H.; Higginson, B. R.; Lloyd, D. R. *Mol. Phys.* **1975**, *29*, 113.
(45) Falcatta, M. F.; Chui, Y.; Jordan, K. D. *J. Phys. Chem.* **2000**, *1044*, 9605.
(46) Vydrov, O. A.; Scuseria, G. E. *J. Chem. Phys.* **2005**, *122*, 184107.
(47) Dutoi, A. D.; Head-Cordan, M. *Chem. Phys. Lett.* **2006**, *422*, 230.
(48) Gopinathan, M. S. *J. Phys. B* **1979**, *12*, 521.
(49) Vydrov, O. A.; Scuseria, G. E.; Perdew, J. P. *J. Chem. Phys.* **2007**, *126*, 154109.
(50) Yanai, T.; Tew, D. P.; Handy, N. C. *Chem. Phys. Lett.* **2004**, *393*, 51.
(51) Chai, J.-D.; Head-Gordon, M. *Phys. Chem. Chem. Phys.* **2008**, *10*, 6615.

JP904056Q